

# Metrological Characterization of Multipartite Continuous-Variable non-Gaussian Entanglement Structure

Mingsheng Tian,<sup>1, 2, \*</sup> Xiaoting Gao,<sup>1, \*</sup> Boxuan Jing,<sup>1</sup> Feng-Xiao Sun,<sup>1</sup> Matteo Fadel,<sup>3</sup> and Qiongyi He<sup>1, 4, 5, 6, †</sup>

<sup>1</sup>*State Key Laboratory for Mesoscopic Physics, School of Physics,  
Frontiers Science Center for Nano-optoelectronics,*

*& Collaborative Innovation Center of Quantum Matter, Peking University, Beijing 100871, China*

<sup>2</sup>*Department of Physics, The Pennsylvania State University, University Park, Pennsylvania, 16802, USA*

<sup>3</sup>*Department of Physics, ETH Zürich, 8093 Zürich, Switzerland*

<sup>4</sup>*Collaborative Innovation Center of Extreme Optics,  
Shanxi University, Taiyuan, Shanxi 030006, China*

<sup>5</sup>*Peking University Yangtze Delta Institute of Optoelectronics, Nantong, Jiangsu 226010, China*

<sup>6</sup>*Hefei National Laboratory, Hefei 230088, China*

Multipartite entanglement is an essential resource for quantum information tasks, but characterizing entanglement structures in continuous variable systems remains challenging, especially in multimode non-Gaussian scenarios. In this work, we introduce a method for detecting multipartite entanglement structures in continuous variable states. By leveraging the quantum Fisher information, we propose a systematic approach to identify feasible operators that capture quantum correlations in multimode non-Gaussian states. We demonstrate the effectiveness of our method on over  $10^5$  randomly generated multimode-entangled quantum states, achieving a high success rate in entanglement detection. Additionally, our method exhibits enhanced robustness against losses by expanding the set of accessible operators. This work provides a general framework for characterizing entanglement structures in diverse continuous variable systems, enabling a number of experimentally relevant applications.

Multipartite entanglement is an essential resource for many quantum computation, sensing and communication protocols [1–10]. Its importance is particularly evident in continuous variable (CV) systems, where multimode Gaussian states, such as squeezed states and cluster states, can be deterministically prepared and controlled [11–13]. However, to achieve an advantage over classical protocols in CV systems, non-Gaussian features are necessary [14]. Non-Gaussian states play a crucial role for quantum computation [15–17], sensing [18–21], and imaging [22, 23]. Strategies to generate and control such states has seen substantial advancements in recent years, including through photon-subtraction [24, 25] and nonlinear operations, such as spontaneous parametric down-conversion (SPDC) [26, 27] and Kerr interactions in microwave cavities coupled superconducting artificial atoms [28–30].

Despite these advancements, accurately characterizing both Gaussian and non-Gaussian multimode entanglement in CV systems continues to present significant challenges [14], e.g. due to the complex correlations appearing among higher-order statistical moments of quadrature field operations. Unlike discrete variable (DV) systems, where entanglement structures are identified based on separable partitions and their sizes [31–35], there is no similarly comprehensive method for CV systems. State-of-the-art techniques in CV systems predominantly analyze bi- and multipartite entanglement through first and second-order moments [36–44]. Since non-Gaussian states involve more complex higher-order correlations, these techniques are mostly limited to the study of Gaussian CV entanglement. Criteria for detecting non-

Gaussian CV entanglement [45–49] can only distinguish entanglement properties of individual partitions and become ineffective with different partitions. This limitation hinders the understanding of complex structures, such as the fully inseparable entanglement structure. Therefore, there is a pressing need to develop a method to characterize the multipartite entanglement structure in non-Gaussian CV systems, filling this significant gap in the field.

Here, we propose a general method to characterize entanglement structure based on quantum metrology tools. Specifically, we systematically determine the operators that can effectively capture complex correlations in multimode systems. Our approach begins with the analytical identification of a convex set of operators, each capable of witnessing specific bi-inseparable entanglement structures across arbitrary quantum states. Since different entanglement structures correlate with distinct convex sets, we then proceed to pinpoint the intersection of these sets. This intersection allows us to identify an optimal operator for witnessing entanglement. Crucially, contrary to previous work where the chosen operator can identify a specific entanglement structure, our method identifies different entanglement structures with the optimal operator, which enables us to efficiently characterize and detect entanglement structures. To demonstrate the practicality and efficiency of our method, we apply it to a broad range of non-Gaussian states generated through various stellar ranks and nonlinear processes, including over  $10^5$  randomly produced quantum states. Furthermore, we examine the robustness of our method in scenarios involving loss, demonstrating that the inclusion of high-

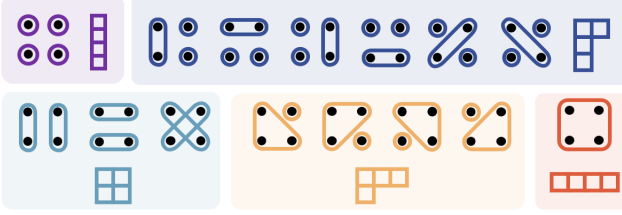


FIG. 1. Graph representation of different multipartite entanglement structures. As illustrated, a system with  $N = 4$  modes can be characterized by 15 different partitions, associated to different distributions of correlations as indicated by the solid circles. Each partition can be graphically represented by a Young tableau, where boxes in each row indicate correlated modes, while vertically stacked boxes indicate separable subsets.

order operators significantly enhances resilience to loss channels. This approach marks the accessible method for witnessing entanglement structure in arbitrary Gaussian and non-Gaussian states, thereby addressing a significant need in CV systems.

*Metrological bound for  $\mathcal{K}$ -partitions.*— We begin discussing the entanglement structure for  $N$  parties. A partition  $\mathcal{K} = \{H_1, H_2, \dots, H_k\}$  separates the total  $N$ -partite system into  $k$  nonempty, disjoint subsets  $H_l$ , where each subset has a size  $N_l$  such that  $\sum_{l=1}^k N_l = N$ . A state  $\hat{\rho}_{\mathcal{K}}$  is  $\mathcal{K}$ -separable if there exists local quantum states  $\hat{\rho}_{H_l}^{(\gamma)}$  for each subset and a probability distribution  $p_{\gamma}$  such that  $\hat{\rho}_{\mathcal{K}} = \sum_{\gamma} p_{\gamma} \hat{\rho}_{H_1}^{(\gamma)} \otimes \dots \otimes \hat{\rho}_{H_k}^{(\gamma)}$ . A partition  $\mathcal{K}$  can be classified in terms of the number and respective sizes of the separable subsets. This can be illustrated graphically by means of Young tableau, as illustrated in Fig. 1 for a 4-mode system.

Using the framework of quantum metrology, it is known that for an arbitrary  $\mathcal{K}$ -separable state  $\hat{\rho}_{\mathcal{K}}$ , the quantum Fisher information (QFI) is bounded by the variances as [43, 46]

$$F_Q(\hat{\rho}_{\mathcal{K}}, \hat{A}) \leq 4\mathcal{V}(\hat{\rho}_{\mathcal{K}}, \hat{A}). \quad (1)$$

Here,  $\hat{A} = \sum_{j=1}^N \hat{A}_j$  with  $\hat{A}_j$  represents a local generator in the reduced state  $\hat{\rho}_j$ ,  $\mathcal{V}(\hat{\rho}_{\mathcal{K}}, \hat{A}) = \sum_{i=1}^k \text{Var}(\hat{\rho}_{H_i}, \sum_{j \in H_i} \hat{A}_j)$ ,  $\text{Var}(\hat{\rho}, \hat{O}) = \langle \hat{O}^2 \rangle_{\hat{\rho}} - \langle \hat{O} \rangle_{\hat{\rho}}^2$  defines the variance, and  $\hat{\rho}_{H_i} = \sum_{\gamma} p_{\gamma} \hat{\rho}_{H_i}^{(\gamma)}$  the reduced state of subsystem  $H_i$ . The explicit expression of the QFI is given by  $F_Q[\hat{\rho}_{\mathcal{K}}, \hat{A}] = 2 \sum_{\substack{k, l \\ p_k + p_l \neq 0}} \frac{(p_k - p_l)^2}{p_k + p_l} |\langle \Psi_k | \hat{A} | \Psi_l \rangle|^2$ , with the spectral decomposition  $\hat{\rho} = \sum_k p_k |\Psi_k\rangle\langle\Psi_k|$  [50]. Since Eq. (1) is a necessary criterion for separability, its violation implies  $\mathcal{K}$ -inseparability.

The right-hand side of the criterion (1) is tailored to detect inseparability within the specific partition  $\mathcal{K}$ . To maximize entanglement detection, one must optimize the operator  $A$  to achieve the largest possible violation of

Eq. (1). Different partitions typically correspond to different operators  $\hat{A}$ . Therefore, if an operator  $\hat{A}$  exists for a quantum state  $\hat{\rho}$  that can capture correlations across all partitions corresponding to a given Young diagram, as illustrated in Fig. 1, it offers a more efficient way to characterize the entanglement structure. To this aim, we propose a general and systematic optimization method to characterize different partitions with the same operator  $\hat{A}$ . The methodology consists of the following steps:

*Step 1.*— *Finding the convex sets of operators witnessing entanglement for each  $\mathcal{K}$ -partition.*

To witness  $\mathcal{K}$ -partite entanglement through inequality (1) the choice of suitable local operators  $\hat{A}_j$  is crucial and dependent on the given state  $\hat{\rho}$ . These operators can be constructed by analytically optimizing over linear combinations of accessible operators forming the set  $\mathbf{S}_j = \{S_j^{(1)}, S_j^{(2)}, \dots\}$  [46]. Specifically, we express  $\hat{A}_j$  as the linear combination

$$\hat{A}_j = \sum_{m=1} c_j^{(m)} \hat{S}_j^{(m)} = \mathbf{c}_j \cdot \mathbf{S}_j. \quad (2)$$

A typical choice for such a set includes local position operators  $\hat{x}_j$  and momentum operators  $\hat{p}_j$ . However, since the states we consider are in general non-Gaussian, simply measuring linear observables is insufficient for characterizing their correlations. We therefore extend the family of accessible operators by incorporating higher-order moments of local quadrature operators, e.g.  $\mathbf{S}_j = [\hat{x}_j, \hat{p}_j, \hat{x}_j^2, \hat{p}_j^2, (\hat{x}_j \hat{p}_j + \hat{p}_j \hat{x}_j)/2]^T$ . The full operator  $\hat{A}(\mathbf{c})$  is then  $\hat{A}(\mathbf{c}) = \sum_{j=1}^N \hat{A}_j = \sum_{j=1}^N \mathbf{c}_j \cdot \mathbf{S}_j$ . According to Eq. (1), the quantity  $W = F_Q[\hat{\rho}_{\mathcal{K}}, \hat{A}] - 4\mathcal{V}(\hat{\rho}_{\mathcal{K}}, \hat{A})$  must be nonpositive when the state is separable. To witness entanglement, we maximize  $W$  by varying  $\mathbf{c}$  to obtain an optimal operator  $\hat{A}(\mathbf{c}^{\text{opt}})$ . This optimization problem can be formulated mathematically by expressing  $W$  in a Rayleigh quotient form  $W(\mathcal{M}, \mathbf{c}) = \frac{\mathbf{c}^T \mathcal{M} \mathbf{c}}{\mathbf{c}^T \mathbf{c}}$  [43]. Here,  $\mathcal{M}$  is a Hermitian matrix associated with the operator set  $\mathbf{S}_j$  and the targeted quantum states (see the supplementary material [51] for details).

To determine the convex sets of operators for  $\mathcal{K}$ -partition inseparability, we decompose the matrix  $\mathcal{M}$  as follows:  $\mathcal{M} = UDU^T$ , where  $U$  is an orthogonal matrix, satisfying  $U^T U = U U^T = I$ , and  $D$  is a diagonal matrix containing the eigenvalues  $\lambda_i$  of  $\mathcal{M}$ . A normalized vector  $\mathbf{c}$  can be expressed by the eigenvectors  $\mathbf{e}_i$ :  $\mathbf{c} = \sum_i n_i \mathbf{e}_i$ . Substituting this into the Rayleigh quotient  $W$ , we obtain:

$$\begin{aligned} W(\mathcal{M}, \mathbf{c}) &= \sum_{ij} n_i n_j \mathbf{e}_i^T U D U^T \mathbf{e}_j \\ &= \sum_{ij} n_i n_j D_{ij} = \sum_i n_i^2 \lambda_i. \end{aligned} \quad (3)$$

This indicates that if there is a subset of eigenvectors  $Q$ , where  $\forall \mathbf{e}_i \in Q, W(\mathcal{M}, \mathbf{e}_i) > 0$ , then any linear combina-

tion  $\mathbf{c} = \sum_i n_i \mathbf{e}_i$  will also satisfy  $W(\mathcal{M}, \mathbf{c}) > 0$ . Therefore, all vectors  $\mathbf{e}_i$  for which  $W(\mathcal{M}, \mathbf{e}_i) > 0$  form convex sets. This completes *Step 1*.

*Step 2.—Determining the intersection of convex sets for different types of entanglement structures.*

For each  $\mathcal{K}$ -partition of the  $N$  parties, the convex sets of operators determined in *Step 1* corresponds to a subspace. Different  $\mathcal{K}$ -partitions will in general generate different subspaces  $Q_j$ , and the overlap of these subspaces  $P = \bigcap_{j=1}^m Q_j$  (if any) indicates a common set of operators that allows us to certify  $\Lambda$ -partition inseparability.

*Step 3.—Find the suitable operator to witness entanglement within the intersection space.*

The operators for detecting entanglement structure can be optimized by maximizing the minimum value of  $W(\mathcal{M}_i, \mathbf{c})$  across all matrices  $\mathcal{M}_i$ ,

$$g = \min\{W(\mathcal{M}_1, \mathbf{c}), W(\mathcal{M}_2, \mathbf{c}), W(\mathcal{M}_3, \mathbf{c}), \dots\}, \quad (4)$$

with  $\mathcal{M}_i$  are associated to each  $\mathcal{K}$ -partition. However, this optimization can be analytically challenging with the existence of different Rayleigh quotients  $W(\mathcal{M}_i, \mathbf{c})$ . To simplify the optimization, we construct a combined function that integrates different  $\mathcal{M}_i$

$$\begin{aligned} f &= \sum_i W(\mathcal{M}_i, \mathbf{c}) = W\left(\sum_i \mathcal{M}_i, \mathbf{c}\right) \\ &= \sum_{i=1}^k \sum_{j=1}^k n_i n_j (\mathbf{p}_i^T M \mathbf{p}_j) = \mathbf{n}^T \mathcal{Q} \mathbf{n}, \end{aligned} \quad (5)$$

where we have now the vector  $\mathbf{c} = \sum_i n_i \mathbf{p}_i$ , with  $\mathbf{p}_i$  being the basis in the intersection space  $P$ , and  $n_i$  are the coefficients to be determined [52]. Here,  $\mathcal{Q}$  is a symmetric matrix with elements  $q_{ij} = \mathbf{p}_i^T M \mathbf{p}_j$ .

The optimal  $\mathbf{c}$  can be found by maximizing the value of  $g$  in Eq. (4). This involves selecting the positive eigenvalues  $\lambda_j$  of  $\mathcal{Q}$  that satisfy  $g > 0$  and then determining the eigenvector corresponding to the optimal  $\lambda_j$  that maximizes  $g$ . This ends *Step 3*.

These three steps provide a general method for finding an operator to witness entanglement for different partitions. In the following, we will apply this methodology to various general CV states (both Gaussian and non-Gaussian), demonstrating its effectiveness in characterizing multipartite entanglement structures.

*Characterizing entanglement structure of random Gaussian and non-Gaussian states.*— The generation of a random CV quantum state  $\hat{\rho}$  begins with a core state  $|C\rangle$  using the stellar formalism [53–55]. A multimode quantum state is then generated by applying an  $m$ -mode random Gaussian unitary operation  $\hat{G}$  to the core state, namely as  $|\psi\rangle = \hat{G}|C\rangle$ . This procedure results in states that includes the most common Gaussian and non-Gaussian states prepared in experiments, such

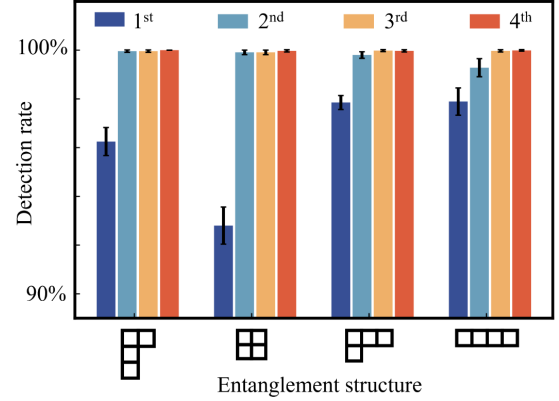


FIG. 2. Multipartite entanglement structure detection. Without loss of generality, we randomly generated  $10^4$  four-mode entangled states for each entanglement structure, classified according to Young diagram. The vertical axis shows the successful rate of detecting this type of entanglement. The color denotes the order of the encoding operators  $\mathbf{S}_j$  in QFI. The error bars represent the standard deviation of the detection rate, calculated by dividing these  $10^4$  states into 10 sets.

as squeezed and photon subtracted states (see details in the supplementary material [51]). The entanglement structure of these random generated multimode states cannot be characterized by the previous criteria based on covariance matrix [36–40] and QFI [43, 47]. The primary limitations of these methods are their inability to detect entanglement across different partitions due to their focus on a specific partition, or their reliance on measuring variances of linear combinations of position and momentum operators, which do not capture non-Gaussian correlations. In contrast, our method based on QFI overcomes these challenges.

To test the effectiveness of our method, We randomly generate 40000 four-mode quantum states (ensuring 10,000 states for each type of entanglement structure). As shown in Fig. 2, our method based on QFI demonstrating a high success rate in detecting entanglement structures. For four modes, using first-order encoding operators  $\hat{A}$  (combinations of  $\hat{x}$  and  $\hat{p}$ ) we can reach over 90% detection rate. By including higher-order operators ( $\hat{x}^2, \hat{p}^2, \hat{x}\hat{p} + \hat{p}\hat{x}, \dots$ ), the successful rate of characterizing entanglement structure increases to almost 100%.

Additionally, the effectiveness of our method is not confined to four-mode systems; Similar results can also be extended to four and five modes. As illustrated in Fig. 3(a), our approach exhibits a high success rate in detecting fully inseparable in different multimodes. For three modes, using first-order encoding operators  $\hat{A}$  (combinations of  $\hat{x}$  and  $\hat{p}$ ), we successfully detect fully inseparable entanglement in around 94.3% of three-mode cases. By incorporating second-order encoding operators ( $\hat{x}^2, \hat{p}^2, \hat{x}\hat{p} + \hat{p}\hat{x}$ ), the successful detecting rate increases

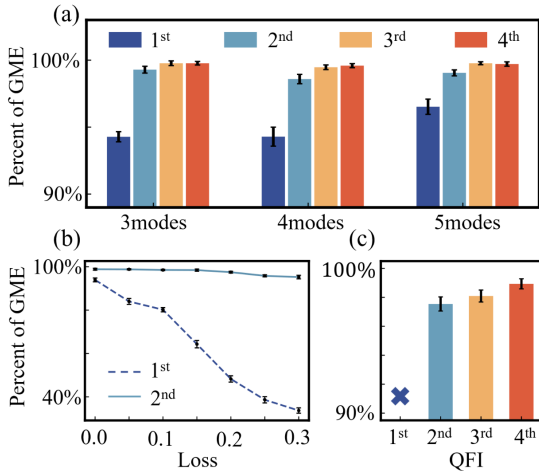


FIG. 3. Witnessing fully inseparable entanglement for different non-Gaussian states. (a) The success rate of detecting entanglement for different multimode cases, where we randomly generated  $10^4$  fully inseparable states of 3, 4, and 5 modes. The color denotes the order of the encoding operators in QFI. The error bars represent the standard deviation of the percentage of detecting fully inseparable states, calculated by dividing these  $10^4$  states into 10 sets. (b) The percentage of detectable fully inseparable states in the presence of channel loss, where the blue and green denote the QFI criterion based on first-order and second-order operators, respectively. (c) The witness of full inseparability using QFI based on the three-photon SPDC process, where we generated  $10^4$  states with random nonlinear strengths and plotted the percentage of detectable full inseparable states using operators of different orders.

to 99.3%. This performance further improves by extending the operator family to higher orders, achieving 99.8% successful rate with fourth-order operators.

Furthermore, we evaluate the performance of our method in the presence of a loss channel. Losses are introduced to the pure entangled state  $|\psi\rangle = \hat{G}|C\rangle$  using a single-mode loss channel  $\hat{L}_i(\eta)$  with efficiency coefficient  $\eta$ , as detailed in Ref. [56]. The state with loss is described by:  $\hat{\rho} = \left(\prod_{i=1}^m \hat{L}_i(\eta_i)\right) \hat{G}|C\rangle\langle C|\hat{G}^\dagger \left(\prod_{i=1}^m \hat{L}_i^\dagger(\eta_i)\right)$ . Increased channel loss ( $1 - \eta$ ) impacts both the entanglement itself and the successful detection rate. As indicated by the blue curve in Fig. 3(b), the percentage of detectable fully inseparable states using first-order QFI decreases with increasing loss. Intriguingly, we demonstrate that extending the analysis to include second-order operators significantly enhances the successful detection rate, showing robustness against channel loss. This improvement is depicted in the green curves of Fig. 3(b).

In addition to examining non-Gaussian states generated from core states, we also explore non-Gaussian states produced by nonlinear processes, such as the three-photon SPDC process. This process has been realized experimentally [26, 27] and has theoretically attracted significant interest due to its challenges in characteriz-

ing its correlations [57–62]. For our analysis, we randomly generated  $10^4$  non-Gaussian states using the three-photon SPDC process, described by the Hamiltonian  $\hat{H} = (\chi_1 \hat{a}^2 + \chi_2 \hat{b}^2 + \chi_3 \hat{c}^2) + h.c.$  Here the parameters  $\chi_i t$  are randomly selected from the interval  $[0, 0.04]$ , and the initial states are vacuum states. As illustrated in Fig. 3(c), the specific form of the three-photon Hamiltonian means that the first-order QFI fails to detect any quantum correlations. In contrast, higher-order QFI successfully identifies entanglement. These results exhibit the versatility of our method across different non-Gaussian states, demonstrating its effectiveness in accurately identifying operators that capture complex non-Gaussian correlations.

In conclusion, we provide a general method for characterizing entanglement for arbitrarily Gaussian and non-Gaussian states. Based on QFI, we establish a criterion and propose a systematic approach to identify entanglement by analytically optimizing operators from accessible family of operators. This method involves three key steps: (i) identifying convex sets of operators that can be used to witness  $\mathcal{K}$ -partition entanglement, (ii) determining the intersection of these sets, and (iii) selecting a suitable operator at the intersection. To verify the accessibility and effectiveness of our method, we randomly generated  $10^5$  states based on core states and nonlinear processes, which demonstrate a very high proportion of success in detecting entanglement structure. Furthermore, we exhibit the advantage of our method in resisting channel loss and detecting non-Gaussian entanglement. This approach provides a systematic way to distinguish entanglement structure for arbitrary states in CV systems, paving the way for further exploration and detection of entanglement in multimode experimental systems.

This work is supported by the National Natural Science Foundation of China (No. 12125402 and No. 12474256), the Innovation Program for Quantum Science and Technology (No. 2021ZD0301500), and Beijing Natural Science Foundation (Grant No. Z240007). M.F. was supported by the Swiss National Science Foundation Ambizione Grant No. 208886, and by The Branco Weiss Fellowship – Society in Science, administered by the ETH Zürich.

\* These authors contributed equally to this work.

† [qiongyihe@pku.edu.cn](mailto:qiongyihe@pku.edu.cn)

- [1] P. van Loock and S. L. Braunstein, Multipartite entanglement for continuous variables: A quantum teleportation network, *Phys. Rev. Lett.* **84**, 3482 (2000).
- [2] N. Gisin, G. Ribordy, W. Tittel, and H. Zbinden, Quantum cryptography, *Rev. Mod. Phys.* **74**, 145 (2002).
- [3] O. Gühne and G. Tóth, Entanglement detection, *Phys. Rep.* **474**, 1 (2009).
- [4] J.-D. Bancal, N. Gisin, Y.-C. Liang, and S. Pironio,

Device-independent witnesses of genuine multipartite entanglement, *Phys. Rev. Lett.* **106**, 250404 (2011).

[5] S. Das, S. Bäuml, M. Winczewski, and K. Horodecki, Universal limitations on quantum key distribution over a network, *Phys. Rev. X* **11**, 041016 (2021).

[6] V. Giovannetti, S. Lloyd, and L. Maccone, Quantum-enhanced measurements: Beating the standard quantum limit, *Science* **306**, 1330 (2004).

[7] H. J. Briegel, D. E. Browne, W. Dür, R. Raussendorf, and M. Van den Nest, Measurement-based quantum computation, *Nat. Phys.* **5**, 19 (2009).

[8] J. Bao, Z. Fu, T. Pramanik, J. Mao, Y. Chi, Y. Cao, C. Zhai, Y. Mao, T. Dai, X. Chen, et al., Very-large-scale integrated quantum graph photonics, *Nat. Photonics* **17**, 573 (2023).

[9] S. Yokoyama, R. Ukai, S. C. Armstrong, C. Sornphiphatphong, T. Kaji, S. Suzuki, J.-i. Yoshikawa, H. Yonezawa, N. C. Menicucci, and A. Furusawa, Ultra-large-scale continuous-variable cluster states multiplexed in the time domain, *Nat. Photonics* **7**, 982 (2013).

[10] I. Frerot, M. Fadel, and M. Lewenstein, Probing quantum correlations in many-body systems: a review of scalable methods, *Rep. Prog. Phys.* **86**, 114001 (2023).

[11] S. Yokoyama, R. Ukai, S. C. Armstrong, C. Sornphiphatphong, T. Kaji, S. Suzuki, J.-i. Yoshikawa, H. Yonezawa, N. C. Menicucci, and A. Furusawa, Ultra-large-scale continuous-variable cluster states multiplexed in the time domain, *Nat. Photonics* **7**, 982 (2013).

[12] U. L. Andersen, J. S. Neergaard-Nielsen, P. van Loock, and A. Furusawa, Hybrid discrete- and continuous-variable quantum information, *Nat. Phys.* **11**, 713 (2015).

[13] S. Armstrong, M. Wang, R. Y. Teh, Q. Gong, Q. He, J. Janousek, H.-A. Bachor, M. D. Reid, and P. K. Lam, Multipartite einstein–podolsky–rosen steering and genuine tripartite entanglement with optical networks, *Nat. Phys.* **11**, 167 (2015).

[14] M. Walschaers, Non-Gaussian quantum states and where to find them, *PRX Quantum* **2**, 030204 (2021).

[15] J. Niset, J. Fiurášek, and N. J. Cerf, No-go theorem for Gaussian quantum error correction, *Phys. Rev. Lett.* **102**, 120501 (2009).

[16] A. Mari and J. Eisert, Positive wigner functions render classical simulation of quantum computation efficient, *Phys. Rev. Lett.* **109**, 230503 (2012).

[17] U. Chabaud and M. Walschaers, Resources for bosonic quantum computational advantage, *Phys. Rev. Lett.* **130**, 090602 (2023).

[18] J. Joo, W. J. Munro, and T. P. Spiller, Quantum metrology with entangled coherent states, *Phys. Rev. Lett.* **107**, 083601 (2011).

[19] H. Strobel, W. Muessel, D. Linnemann, T. Zibold, D. B. Hume, L. Pezzè, A. Smerzi, and M. K. Oberthaler, Fisher information and entanglement of non-Gaussian spin states, *Science* **345**, 424 (2014).

[20] F. Hanamura, W. Asavanant, S. Kikura, M. Mishima, S. Miki, H. Terai, M. Yabuno, F. China, K. Fukui, M. Endo, and A. Furusawa, Single-shot single-mode optical two-parameter displacement estimation beyond classical limit, *Phys. Rev. Lett.* **131**, 230801 (2023).

[21] M. Tian, Y. Xiang, F.-X. Sun, M. Fadel, and Q. He, Characterizing multipartite non-Gaussian entanglement for a three-mode spontaneous parametric down-conversion process, *Phys. Rev. Appl.* **18**, 024065 (2022).

[22] D. Liu, M. Tian, S. Liu, X. Dong, J. Guo, Q. He, H. Xu, and Z. Li, Ghost imaging with non-Gaussian quantum light, *Phys. Rev. Appl.* **16**, 064037 (2021).

[23] I. Karuseichyk, G. Sorelli, M. Walschaers, N. Treps, and M. Gessner, Resolving mutually-coherent point sources of light with arbitrary statistics, *Phys. Rev. Res.* **4**, 043010 (2022).

[24] N. Namekata, Y. Takahashi, G. Fujii, D. Fukuda, S. Kurimura, and S. Inoue, Non-gaussian operation based on photon subtraction using a photon-number-resolving detector at a telecommunications wavelength, *Nature Photonics* **4**, 655 (2010).

[25] Y.-S. Ra, A. Dufour, M. Walschaers, C. Jacquard, T. Michel, C. Fabre, and N. Treps, Non-Gaussian quantum states of a multimode light field, *Nat. Phys.* **16**, 144 (2020).

[26] C. W. S. Chang, C. Sabín, P. Forn-Díaz, F. Quijandriá, A. M. Vadiraj, I. Nsanzineza, G. Johansson, and C. M. Wilson, Observation of three-photon spontaneous parametric down-conversion in a superconducting parametric cavity, *Phys. Rev. X* **10**, 011011 (2020).

[27] J. Douady and B. Boulanger, Experimental demonstration of a pure third-order optical parametric downconversion process, *Opt. Lett.* **29**, 2794 (2004).

[28] C. Wang, Y. Y. Gao, P. Reinhold, R. W. Heeres, N. Ofek, K. Chou, C. Axline, M. Reagor, J. Blumoff, K. M. Sliwa, L. Frunzio, S. M. Girvin, L. Jiang, M. Mirrahimi, M. H. Devoret, and R. J. Schoelkopf, A Schrödinger cat living in two boxes, *Science* **352**, 1087 (2016).

[29] M. Bild, M. Fadel, Y. Yang, U. von Lüpke, P. Martin, A. Bruno, and Y. Chu, Schrödinger cat states of a 16-microgram mechanical oscillator, *Science* **380**, 274 (2023).

[30] S. Marti, U. von Lüpke, O. Joshi, Y. Yang, M. Bild, A. Omahen, Y. Chu, and M. Fadel, Quantum squeezing in a nonlinear mechanical oscillator, *Nat. Phys.* [10.1038/s41567-024-02545-6](https://doi.org/10.1038/s41567-024-02545-6) (2024).

[31] P. Hyllus, W. Laskowski, R. Krischek, C. Schwemmer, W. Wieczorek, H. Weinfurter, L. Pezzé, and A. Smerzi, Fisher information and multiparticle entanglement, *Phys. Rev. A* **85**, 022321 (2012).

[32] G. Tóth, Multipartite entanglement and high-precision metrology, *Phys. Rev. A* **85**, 022322 (2012).

[33] Z. Ren, W. Li, A. Smerzi, and M. Gessner, Metrological detection of multipartite entanglement from young diagrams, *Phys. Rev. Lett.* **126**, 080502 (2021).

[34] M. Fadel, B. Yadin, Y. Mao, T. Byrnes, and M. Gessner, Multiparameter quantum metrology and mode entanglement with spatially split nonclassical spin ensembles, *New J. Phys.* **25**, 073006 (2023).

[35] H. Lu, Q. Zhao, Z.-D. Li, X.-F. Yin, X. Yuan, J.-C. Hung, L.-K. Chen, L. Li, N.-L. Liu, C.-Z. Peng, Y.-C. Liang, X. Ma, Y.-A. Chen, and J.-W. Pan, Entanglement structure: Entanglement partitioning in multipartite systems and its experimental detection using optimizable witnesses, *Phys. Rev. X* **8**, 021072 (2018).

[36] L.-M. Duan, G. Giedke, J. I. Cirac, and P. Zoller, Inseparability criterion for continuous variable systems, *Phys. Rev. Lett.* **84**, 2722 (2000).

[37] R. Simon, Peres-horodecki separability criterion for continuous variable systems, *Phys. Rev. Lett.* **84**, 2726 (2000).

[38] P. van Loock and A. Furusawa, Detecting genuine multipartite continuous-variable entanglement, *Phys. Rev. A* **67**, 052315 (2003).

[39] A. S. Coelho, F. A. S. Barbosa, K. N. Cassemiro, A. S. Villar, M. Martinelli, and P. Nussenzveig, Three-color entanglement, *Science* **326**, 823 (2009).

[40] R. Y. Teh and M. D. Reid, Criteria for genuinen-partite continuous-variable entanglement and einstein-podolsky-rosen steering, *Phys. Rev. A* **90**, 062337 (2014).

[41] S. Gerke, J. Sperling, W. Vogel, Y. Cai, J. Roslund, N. Treps, and C. Fabre, Multipartite entanglement of a two-separable state, *Phys. Rev. Lett.* **117**, 110502 (2016).

[42] C. Weedbrook, S. Pirandola, R. García-Patrón, N. J. Cerf, T. C. Ralph, J. H. Shapiro, and S. Lloyd, Gaussian quantum information, *Rev. Mod. Phys.* **84**, 621 (2012).

[43] M. Gessner, L. Pezzè, and A. Smerzi, Entanglement and squeezing in continuous-variable systems, *Quantum* **1**, 17 (2017).

[44] R. Y. Teh, M. Gessner, M. D. Reid, and M. Fadel, Full multipartite steering inseparability, genuine multipartite steering, and monogamy for continuous-variable systems, *Phys. Rev. A* **105**, 012202 (2022).

[45] J. Sperling and W. Vogel, Multipartite entanglement witnesses, *Phys. Rev. Lett.* **111**, 110503 (2013).

[46] M. Gessner, L. Pezzè, and A. Smerzi, Efficient entanglement criteria for discrete, continuous, and hybrid variables, *Phys. Rev. A* **94**, 020101(R) (2016).

[47] Z. Qin, M. Gessner, Z. Ren, X. Deng, D. Han, W. Li, X. Su, A. Smerzi, and K. Peng, Characterizing the multipartite continuous-variable entanglement structure from squeezing coefficients and the fisher information, *npj Quantum Inf.* **5**, 3 (2019).

[48] M. Fadel and M. Gessner, Entanglement of Local Hidden States, *Quantum* **6**, 651 (2022).

[49] D. Barral, M. Isoard, G. Sorelli, M. Gessner, N. Treps, and M. Walschaers, Metrological detection of entanglement generated by non-gaussian operations, *New Journal of Physics* **26**, 083012 (2024).

[50] S. L. Braunstein and C. M. Caves, Statistical distance and the geometry of quantum states, *Phys. Rev. Lett.* **72**, 3439 (1994).

[51] See Supplemental Material for further details about state generations and more examples for characterizing multi-mode entanglement.

[52] The intersection Hilbert space  $P$  can also be substituted to a larger Hilbert space in Eq. (7).

[53] U. Chabaud, D. Markham, and F. Grosshans, Stellar representation of non-Gaussian quantum states, *Phys. Rev. Lett.* **124**, 063605 (2020).

[54] U. Chabaud, G. Ferrini, F. Grosshans, and D. Markham, Classical simulation of Gaussian quantum circuits with non-Gaussian input states, *Phys. Rev. Res.* **3**, 033018 (2021).

[55] U. Chabaud and S. Mehraban, Holomorphic representation of quantum computations, *Quantum* **6**, 831 (2022).

[56] M. Eaton, C. González-Arciniegas, R. N. Alexander, N. C. Menicucci, and O. Pfister, Measurement-based generation and preservation of cat and grid states within a continuous-variable cluster state, *Quantum* **6**, 769 (2022).

[57] E. A. R. Gonzalez, A. Borne, B. Boulanger, J. A. Levenson, and K. Bencheikh, Continuous-variable triple-photon states quantum entanglement, *Phys. Rev. Lett.* **120**, 043601 (2018).

[58] Y. Shen, S. M. Assad, N. B. Grosse, X. Y. Li, M. D. Reid, and P. K. Lam, Nonlinear entanglement and its application to generating cat states, *Phys. Rev. Lett.* **114**, 100403 (2015).

[59] A. Agustí, C. W. S. Chang, F. Quijandría, G. Johansson, C. M. Wilson, and C. Sabín, Tripartite genuine non-Gaussian entanglement in three-mode spontaneous parametric down-conversion, *Phys. Rev. Lett.* **125**, 020502 (2020).

[60] D. Zhang, Y. Cai, Z. Zheng, D. Barral, Y. Zhang, M. Xiao, and K. Bencheikh, Non-Gaussian nature and entanglement of spontaneous parametric nondegenerate triple-photon generation, *Phys. Rev. A* **103**, 013704 (2021).

[61] D. Zhang, D. Barral, Y. Cai, Y. Zhang, M. Xiao, and K. Bencheikh, Hierarchy of nonlinear entanglement dynamics for continuous variables, *Phys. Rev. Lett.* **127**, 150502 (2021).

[62] D. Zhang, D. Barral, Y. Zhang, M. Xiao, and K. Bencheikh, Genuine tripartite non-Gaussian entanglement, *Phys. Rev. Lett.* **130**, 093602 (2023).